Geometry of Patchy Snowcovers

K. SHOOK, D.M. GRAY
Division of Hydrology
Department of Agricultural and Bioresource Engineering
University of Saskatchewan
Saskatoon, Saskatchewan S7N 0W0 Canada

J.W. POMEROY
National Hydrology Research Institute
Environment Canada
11 Innovation Boulevard
Saskatoon, Saskatchewan S7N 3H5 Canada

ABSTRACT

The influence of the spatial variation in snowcover water equivalent on areal snow-cover depletion and the geometry of snow patches that form during the ablation of shallow, seasonal snowcovers in open environments is discussed. A simplified snowpack ablation simulation is used to demonstrate that the fractal structure of the snowcover water equivalent causes soil and snow patches to possess fractal characteristics. This program is a distributed, grid-square model that uses a synthetically-generated snowcover and includes an algorithm for approximating the effects of local advection on melt. Fractal dimension(s) of snow patches produced by the model are shown to agree closely with the dimensions of natural ablated snowcovers determined from analyses of aerial photographs.

INTRODUCTION

Information on the temporal variation in snow-covered area of watershed during melt is requisite for accurate predictions of runoff. In open environments, the extent of the gross area of a watershed that is snow-covered affects runoff primarily in two ways: (a) it influences the melt rate, because patches of bare ground affect the energy balance of the snow field, and (b) it governs the contributing area of runoff. The highest rate of meltwater production on a watershed will occur when the product of the average melt rate and snow-covered area is a maximum.

Large areas of bare ground within a snow field significantly alter its energy balance. Bare ground, having a lower albedo than snow, absorbs larger amounts of solar radiation and heats more quickly. Local advection of energy from the bare patches and the turbulent transfer of latent and sensible heat to adjacent snow surfaces increase the melt rate. Melting due to advection is most noticeable along the edges of snow patches. Small snow patches are dominated by turbulent melt throughout the season, or until they disappear; larger snow fields are dominated by radiation melt early in the season and turbulent melt late in the season as they decrease in area.

For a specific melt rate, less meltwater is generated over a watershed when it is partly snow-covered than if completely-covered. Erickson et al. (1978) reported strong correlations between daily snowmelt runoff, mean daily air temperature and extent of snowcover on small watersheds in the Canadian prairies. Martinec and Rango (1986), warn against compensating a meltwater difference that arises from erroneous snowcover information by "optimizing" the melt factor used to calculate snowmelt.

Geometry of Ablating Snowpacks

Shook et al. (1993) applied image analyses to aerial photographs taken during snowmelt on two small watersheds: one located in the Canadian Prairies, the other in the alpine region of the Austrian Alps. They found that the soil and snow patches that form during ablation behave as fractal objects. That is, they have no characteristic size or scale and their quantity of roughness remains constant under increasing magnification. This latter property is know as self-similarity. The perimeter-area and area-frequency characteristics can be

described by power equations (Mandelbrot, 1983):

Perimeter-Area Relationship

$$P = kA^{\frac{D_P}{2}}, \text{ and} \qquad [1]$$

where   P = perimeter,
        k = constant,
        A = area, and
        D_P = fractal dimension (values
            of $D_P > 1.0$).

Korčak's Law

Korčak's law is a rule of thumb that has been found to apply to many fractal systems. The law states that the areas of natural fractal objects will follow a hyperbolic size distribution, i.e.,

$$F(A) = cA^{-\frac{D_K}{2}}, \ A \geq A_{min}, \qquad [2]$$

where   F(A) = fraction of the number of objects
                with a size equal to or greater
                than area, A,
        c = the area of the smallest
                resolution cell, and
        D_K = fractal dimension.

D_K indexes the degree of concentration of area. A small value indicates that most of the area is concentrated in only a few objects; a large value indicates a more uniform distribution of areas.

On the basis of their findings Shook et al. (1993) concluded: (a) soil and snow patches have the same fractal dimension, and (b) snow patches are not random and their size distribution is predictable. When the fractal dimension is known, the perimeter length and relative frequency of patches of specific size can be estimated by Eqs. 1 and 2. This information is required for assessing the influence of advective energy transfers on melting of patchy snowcovers.

Areal Depletion Curves

An areal-depletion curve is often used to correct quantities of melt and runoff, calculated assuming complete snowcover on a basin, for the fraction of the basin area that is snow-covered. Because areal-depletion is strongly affected by the structure (depth and spatial distribution) of the snowcover water equivalent, SWE, numerous studies have used this parameter as the basis for modelling the process (e.g., U.S. Army Corps of Engineers, 1956; Anderson, 1973; Martinec, 1985). Once the relation

between the areal extent and the areal water equivalent of snowcover is known, the fraction of a basin that is snow-covered is approximated from estimates of the amount of melt.

Dunne and Leopold (1978), Ferguson (1984), Buttle and McDonnell, (1987) and Donald (1992), apply one-dimensional melt rates to the distribution of SWE to model the areal extent of snowcover on a basin at various stages of melt. A depletion curve developed in this manner does not include the effects of: (a) local advection on melt, (b) changes in the geometry of the soil and snow patches on the advective component, (c) changes in the albedo of snow due to metamorphism, or (d) changes to the energetics of snowmelt due to the penetration of solar radiation through snow to the underlying ground.
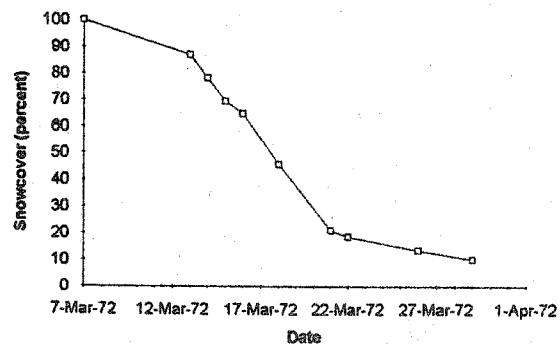

Figure 1. Depletion in snow-covered area on a prairie watershed due to ablation - Smith Tributary, Fiske, SK, 1972.

Figure 1 typifies the depletion in snow-covered area on a prairie watershed due to ablation. The curve has a "sigmoidal" shape in which lower rates of depletion at the beginning and end of melt bound a period when the area of snowcover decreases more rapidly. Figure 2 shows the cumulative frequency curve of snow water equivalent derived from measurements from level fallow and stubble fields in a prairie landscape. Using these data, the important role of the distribution of the water equivalent of a snowcover in areal snowcover depletion can be demonstrated by simple simulation. Figure 3 shows area-depletion curves derived by applying "advanced", "uniform" and "delayed" one-dimensional melt patterns to an array of elements having the distribution of water equivalent given by Fig. 2. Each depletion curve has a sigmoidal shape, independent of melt pattern. Only a few shallow elements (the right side of the frequency distribution) are cleared at the beginning of

simulated melt. The majority of elements are cleared by melting from points whose water equivalent fall within mid-range. A few deep elements (the left side of the frequency distribution) retain snowcover for many intervals. Increasing or decreasing the melt rate shifts (advances or delays) and changes the slope of the curve, but does not alter its basic shape:
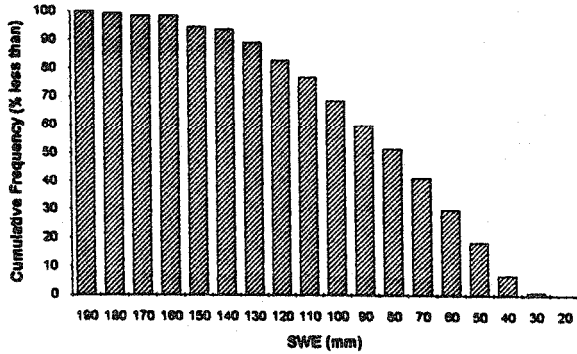

Figure 2. Cumulative frequency distribution of SWE on level fields of fallow and stubble in a prairie landscape, Saskatoon, SK, 1980.
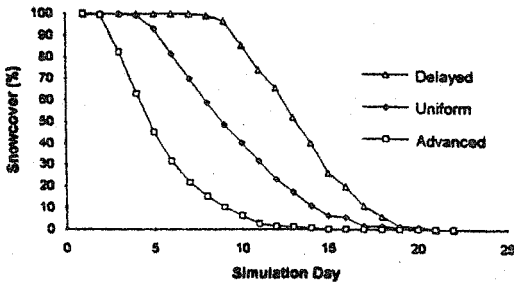

Figure 3. Areal-depletion curves by one-dimensional melt patterns applied to an array with the SWE-distribution in Fig. 2

SPATIAL DISTRIBUTION OF SNOWCOVER WATER EQUIVALENT

An understanding of the development of soil and snow patches of ablating snowcovers as fractals is required for synthesizing the patches in small-scale models of ablation. In this paper it is assumed: (a) the fractal characteristics of soil and snow patches are the result of the spatial variation in the snowcover water equivalent, SWE, and (b) the distribution in SWE is fractal.

There is evidence that the ground surface is generally fractal (Burrough, 1981). Therefore, any

completely-uniform bed of material having a smooth surface that covers the ground would be fractal in its thickness. Also, since the surfaces of deposits of wind-transported snow are highly irregular, the SWE is likely to behave as a fractal. Shook (1993) applied the Hurst exponent (Feder, 1988) to test the fractal structure of snow depth. The Hurst exponent, H, reflects the sensitivity of the variation of data from its mean to sample size. It was originally developed to index autocorrelation in data sets. H = ~0.5 suggests the data is random; H>0.5 suggests the data is fractal. Small-scale surveys of snow depth on relatively-flat fields of fallow and wheat stubble in a prairie landscape produced values for H varying from 0.53 to 1.03 (average H = 0.75). On the basis of these findings Shook (1993) concluded that snow depths are generally fractal. Because SWE is directly related to snow depth (by calculation) and because deeper wind-deposited snow is denser snow (Tabler and Schmidt, 1986) it is unlikely that the fractal dimension for water equivalent will differ appreciably from that for depth. This is especially true if the variability in snow density is less than that of snow depth.

That snow depth appears to be fractal at small scales supports the propositions: (a) the formation of natural snow patches during ablation is due to the spatial variation in the water equivalent of a snowcover and (b) the departure of large snow patches from Korčak's law (Shook et al., 1993) is related to scale. At small scales, the fractal structure of the SWE should cause a snowcover to ablate as a fractal object, i.e., retain its' self-similarity. If the fractal character of snow depth is a property of the snowcover, and poorly-related to large-scale differences in topography of the underlying land surface, this would explain why snowcovers in widely-different landscapes show similar behaviours. Large scales, dominated by landscape topography, form snowcovers that may be fractal, may only be fractal at larger scales, or may have a different fractal dimension. The larger soil and snow patches produced by these large-scale effects will therefore behave differently from the smaller patches.

MODELLING SNOWPACK ABLATION

Simplified Model

A Simplified Snowpack Ablation Simulation, SSAS, was developed to model snowcover ablation. The objective of SSAS is to reproduce the geometry of natural soil and snow patches by using

approximations of the actual energy transfer functions.

SSAS is a distributed, grid-square model. Each element in the grid is assigned a predetermined depth and density of snow. Melt fluxes are applied to a model snowpack to cause melting. As areas of bare ground appear, some of the solar energy they absorb is transferred to the atmosphere. As the air moves downwind over fetches of bare soil, additional amounts of energy are transferred until the air reaches the upwind edges of patches of snow. At the leading edges of snow, the direction of the turbulent energy transfers is reversed and heat is added to the snow patches. Because the system incorporates the areal distribution of snowmelt, SSAS is a three dimensional model.

SSAS Algorithms

No scales are used in SSAS because: (a) SSAS is intended to establish the viability of a particular type of modelling and does not represent any particular location; (b) the ablation process appears to be fractal over a large range of scales, therefore the program should be valid for a wide range in size; and (c) the program is intended to produce fractal results, therefore the introduction of artificial characteristic lengths is generally to be avoided.

SSAS is constructed of several modules that are executed linearly during each iteration. The program begins with a completely snow-covered area and iterates until the snowcover is less than one percent of the modelled area. The structure of the program blocks is shown in Fig. 4. The functioning of each block is described below.

Get Run Parameters

The run parameters are input by the program operator at the beginning of each run. Generally, the parameters determine the methods for the construction of the synthetic snowpack and the magnitudes of the melt rates and energy exchanges.

Set-up Arrays

The most important component of the program is the array, **DEPTH**, which contains up to 200 x 200 elements. **DEPTH** holds the values of SWE used by the model. Each array element is mapped to a pixel on the screen, providing a visual display of the melt sequence. If the snow water equivalent of an array element is less than a user-defined threshold, the element is empty of snow and a black pixel will be plotted on the screen. If the value is greater than the threshold, a white pixel is plotted.
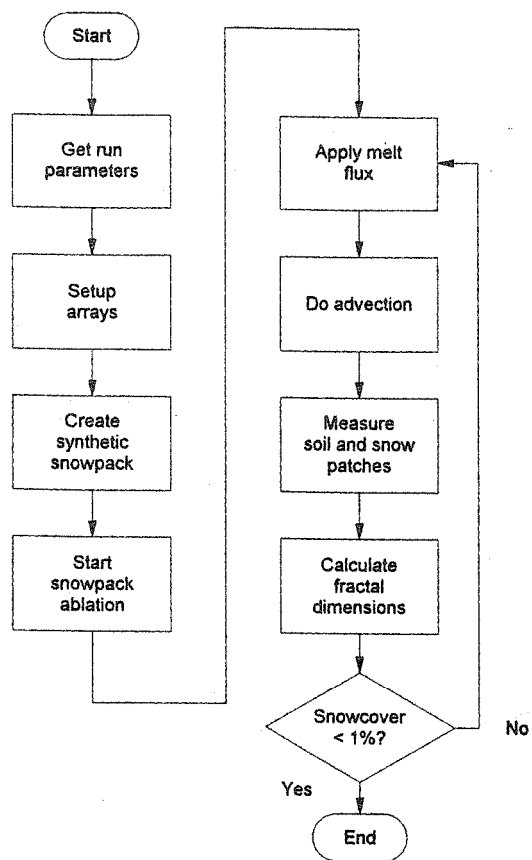

Figure 4. Structure of Simplified Snowpack Ablation Simulation (SSAS) Program.

Create Synthetic Snowpack

A distribution of SWE of a synthetic snowcover is generated using a technique known as the fractal sum of pulses, FSP, which was developed by Lovejoy and Mandelbrot (1985) for modelling clouds and rainfall. Sets of pulses (collections of array elements) are chosen to fit a pre-determined distribution. The dimensions of each pulse are determined by a biased pseudo-random process. According to Lovejoy and Mandelbrot, it is necessary for the pulse sizes and values to be hyperbolically-distributed to generate a fractal object. Each array element in each pulse is assigned a value, again according to a distribution. The values of the pulse elements may be positive or negative. The pulses are then placed at a random location within the final array. As each pulse is placed within the array, the value of the pulse is added to the previous value of the array element. The process is repeated for the desired number of pulses.

The FSP process used to synthesize a snowcover placed "cylinders", i.e., round collections of array

elements, in the array. Shook (1993) gives a program listing for this algorithm. Several parameters are requested from the user to generate the FSP surface. They include: the number of circular pulses, the maximum pulse radius permitted, the exponent for the hyperbolic diameter and depth relationships and the cylinder aspect ratio (of cylinder height to radius). As demonstrated in later discussions, snowpacks generated by this procedure possess fractal properties.

Start Snowpack Ablation

Snowpack ablation is an iterative process. In each iteration the simulated snowpack is subjected to melt fluxes and the resulting soil and snow patches are measured. No attempt is made to measure the soil patches until at least 1% of the model area is snow-free.

Apply Melt Flux

The melt flux is assumed constant for each time step. A constant "depth" of melt (input by the user) is subtracted from all elements whose "depth" is greater than zero, at each iteration of the program.

Do Advection

If the SWE of an element is zero, it is assumed that a portion of the energy flux it receives will be used as sensible heat, which in turn, will be transported downwind by the atmosphere and advected to an adjacent snow patch. The amount of energy available for local advection is simulated by multiplying the melt flux by a user-specified factor. Only part of this energy is transferred and the fraction is specified by the user in terms of the number of array elements that are designated as required for the transfer of the total energy available for advection from one element. That is, if the user specifies 5 elements as the length required to effect the transfer of 100% of the energy available, then each bare element will contribute 1/5 of its available supply. Therefore, the longer the fetch (up to the maximum specified by the user), the greater the quantity of energy advected. The simulated energy transfer is linear, whereas the actual process is non-linear (Weisman, 1977).

SSAS assumes that wind occurs only in the direction of the four main compass points. In each time step, the wind direction is constant and air moves once across the array. This may cause a characteristic length in that the time step is related by the wind velocity to the travel distance.

When the simulated wind reaches an array element containing snow, the energy contained in the air is transferred to the snowpack and reduces its water equivalent by a corresponding amount of melt. Advective energy is distributed uniformly over the snow fetch.

Measure Soil and Snow Patches

The primary output of SSAS is the display of the array **DEPTH** that is mapped to the screen. Displaying the appearance of the snowpack provides the operator a visual display by which to judge the realism of the simulation. Analysis of the patch geometry requires the measurements of the perimeters and areas of the patches and the calculation of the fractal dimensions, D_P and D_K.

The perimeter of each patch is measured with a "bug", a small array (2x2 elements) that "walks" around the outside of the patch by examining the geometry of the edge of the patch. The principle of using a bug to trace an irregular outline is well-known in image processing applications (Rosenfeld and Kak, 1982). As the bug walks around the edge of the patch, it counts the number of elements in the patch perimeter and the location of each edge element. When the bug returns to its original starting point, the tracing of the patch is complete.

Measuring the area involves determinations of the maximum and minimum array columns of each array line of the patch. The area of the patch is determined by counting the number of patch elements on each line between the maximum and minimum array columns.

Calculate Fractal Dimensions

The patch perimeters and areas are stored in separate arrays as they are determined. When all patches have been found, the fractal dimensions, D_P and D_K, are calculated. The perimeter, area and F(A) are transformed into their logarithmic values and least-squares lines fitted to the transformed data following procedures described by Press et al. (1986).

The iterations of snow ablation are repeated until 99% of the model area is snow-free. This threshold was set to prevent errors that would have been generated if the program had tried to measure non-existent snow patches.

RESULTS OF ABLATION SIMULATION

Figure 5 plots normalized values of the perimeters and areas for snow patches: (a) generated by the model (SSAS), (b) determined from image analyses of aerial photographs of a field of summer
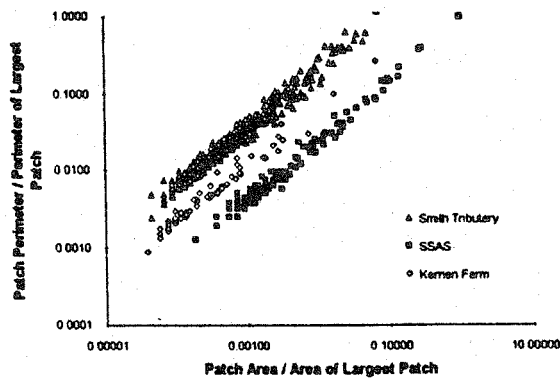
Figure 5. Normalized perimeter-area relationships for snow patches from SSAS, fallow field and Smith Tributary with ~50% snowcover.
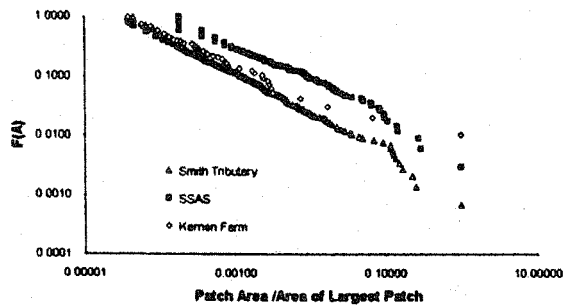

Figure 6. Normalized area-frequency relationships for snow patches from SSAS, fallow field and Smith Tributary with ~50% snowcover.

fallow and (c) determined from analyses of aerial mosaics of a small watershed in western Saskatchewan (Smith Tributary). Figure 6 shows corresponding normalized plots of the size - frequency distribution for modelled and natural patches. These data represent the case when the respective arreas are about 50% snow-covered.

An appreciation of the differences in topography of the fallow field and Smith Tributary can be obtained from Figs. 7 and 8. The fallow field is a relatively-flat, 4.5-ha parcel of land that is denuded of vegetation. Smith Tributary is a catchment with a surface drainage area of about 1.9 km². Its main drainageways are deeply-incised and are subject to preferential accumulation of wind-transported snow. The primary vegetation on the channel slopes are Prairie grass and shrubs. The watershed drains an upland area of flat and gently-moderately rollingtopography that is under cultivation for the production of cereal grains by dryland farming

Figure 7. Aerial photograph of fallow field at Kernen Farm, Saskatoon, SK.
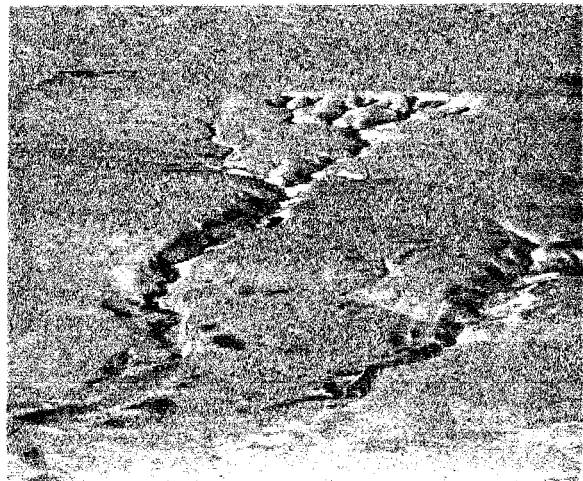

Figure 8. Aerial photograph of Smith Tributary, Fiske, SK.

practices.

The data in Figs. 5 and 6 show that the perimeter-area and size-distribution characteristics of the modelled and natural snowcovers exhibit similar trends. For example, the perimeter - area relationships are linear over a wide range of patch size and the size distributions of small patches generally follow Korčak's law whereas the larger patches depart from the linear association. Note: displacements of the curves in the vertical and horizontal directions are due to differences in the perimeter and the area of the largest patch used to normalize the plots for the various cases.

The fractal dimensions (Eqs. 1 and 2) of snow patches produced by the model and those monitored on the fallow field and the Smith Tributary are

94

listed in Table 1. As expected, since the model and the fallow field are essentially flat planes, there is closer agreement in the dimensions of the patches of these units than in the dimensions of patches for the model and Smith Tributary. The larger values of D_p and D_K for the catchment indicate: (a) the edges of the patches are rougher, i.e., for a patch of given size the perimeter length is longer, and (b) the distribution of areas of patches is more uniform.

Table 1. Fractal dimensions of model and natural snowcovers.

Unit	Fractal Dimensions	
	D_P	D_K
Model (SSAS)	1.46	1.13
Fallow Field	1.46	1.20
Smith Tributary	1.58	1.32

Nevertheless, the agreement in fractal dimensions for model and catchment snow patches is exceptional considering: (a) the model parameters were not optimized to "best" fit the natural data, (b) the large dissimilarities in topography, vegetation and other landscape features of model and proto-type systems, and (c) the effects of differences in hydrological processes, e.g. melt rates and advection, are ignored. Shook (1993) discusses a number of other factors that may have contributed to the differences such as: method of measuring patch geometry, size of model snowpack, measurement precision of image analyses system and quality of aerial photographs. On the basis of these results it is suggested that the areal-depletion of snowcover and the geometry of snow patches that form during ablation are primarily due to the frequency distribution and fractal structure of the snow water equivalent.

SUMMARY

The areal depletion of snowcover during ablation in an open prairie environment is strongly affected by the spatial variation in the water equivalent of a snowcover. To demonstrate the effect, a one-dimensional melt model is applied to an array of elements in which the water equivalent is assigned the frequency distribution of natural snowcover. The general shape of "simulated" depletion curve(s) closely parallel the profile of areal depletion of snowcover monitored in the field.

Evidence is provided which suggests that at small scales the spatial distribution of the water equivalent of a snowcover is fractal. It is assumed that it is the fractal structure of the water equivalent that causes soil and snow patches to possess fractal characteristics. This assumption is verified by comparing the fractal dimension(s) of snow patches produced by a simplified ablation simulation, SSAS, to the dimensions of patches monitored on a relatively flat field of fallow and on a small water-shed. The program, SSAS, is described. It is a distributed, grid-square model that includes an algorithm for approximating the effects of local advection on melt and uses synthetic snow data generated by a technique known as the fractal sum of pulses. The fractal dimensions calculated from the perimeter-area relationships of the patches for the model, fallow field and watershed were 1.46, 1.46 and 1.58 respectively; the dimensions calculated from the size-frequency characteristics of the patches were 1.13, 1.20 and 1.32 respectively.

LITERATURE CITED

Anderson, E.A., 1973. National weather service river forecast system - snow accumulation and. ablation model. NOAA Tech. Memo. NWS HYDRO-17, U.S. Dept. Commer., Washington, D.C.

Burrough, P.A., 1981. Fractal dimensions of land-scapes and other environmental data. Nature 294:240-242.

Buttle, J.M. and J.J. McDonnell, 1987. Modelling the areal depletion of snowcover in a for-ested catchment. J. Hydrol. 90:43-60.

Donald, J.R. 1992. Snowcover depletion curves and satellite snowcover estimates for snowmelt runoff modelling. Ph.D Thesis, Univ. Waterloo, Waterloo, ON, 232 pp.

Dunne, T. and L.B. Leopold, 1978. Water in Environmental Planning. Freeman, San Francisco, CA.

Erickson, D.E.L., W. Lin and H. Steppuhn, 1978. Indices for estimating Prairie runoff from snowmelt. Pap. presented to Seventh Symp. Water Studies Institute, Applied Prairie Hydrol., Saskatoon, SK.

Feder, J., 1988. Fractals. Plenum Press, New York, NY.

Ferguson, R.J., 1984. Magnitude and modelling of snowmelt in the Cairngorm mountains. Hydrol. Sci. J. 29:49-62.

Lovejoy, S. and B.B. Mandelbrot, 1985. Fractal

properties of rain, and a fractal model.
Tellus. 37A:209-232.

Mandelbrot, B.B., 1983. The Fractal Geometry of
Nature. W.H. Freeman and Co., New York,
NY.

Martinec, J., 1985. Snowmelt-runoff models for
operational forecasts. Nordic Hydrol.
16:129-136.

Martinec, J. and A. Rango, 1986. Parameter values
for snowmelt runoff modeling. J. Hydrol.
84:197-219.

Press, W.H., B.P. Flannery, S.A. Teukolsky, and
W.T. Vettering, 1986. Numerical Recipes.
Cambridge University Press, Cambridge,
UK.

Rosenfeld, A. and A. Kak, 1982. Digital Signal
Processing. Academic Press Inc., Orlando,
FL.

Shook, K., 1993. Fractal geometry of snowpacks
during ablation. M.Sc. Thesis, Univ. Sask.,
Saskatoon, SK, 178 pp.

Shook, K., D.M. Gray and J.W. Pomeroy, 1993.
Temporal variation in snowcover area dur-
ing melt in Prairie and Alpine environ-
ments. Special Issue Nordic Hydrology,
(in press).

Tabler, R.D. and R.A. Schmidt, 1986. Snow ero-
sion, transport and deposition. Proc. Symp.
Snow Management for Agriculture (H.
Stepphun and W. Nicholaichuk, eds.) Great
Plains Agricultural Council Pub. 120,
Univ. Nebr., Lincoln, NB, pp. 12-58.

U.S. Army Corps of Engineers, 1956. Snow
Hydrology: Summary Report of the Snow
Investigations. North Pacific Division,
Corps of Engineers, U.S. Army, 210 Cus-
tom House, Portland, OR. 437 pp.

Weisman, R., 1977. Snowmelt: a two-dimensional
turbulent diffusion model. Water Resour.
Res. 13(2):337-342.